Accepted manuscript. Published in Géotechnique (2016). Version of record: https://doi.org/10.1680/jgeot.15.P.119. This is the authors' final version after peer review. Please cite the published article.

Grainsize dependence of yielding in granular soils interpreted using fracture mechanics, breakage mechanics, and Weibull statistics

Y.D. ZHANG[1], G. BUSCARNERA[1], I. EINAV[2]

ABSTRACT

The macroscopic yield pressure of brittle granular soils is experimentally known to depend on the size of soil particles. In this paper this connection is established theoretically within a unified framework that integrates principles of fracture mechanics, breakage mechanics, and Weibull's weakest link theory. In particular, the work input at which a granular continuum begins to comminute is linked to the specific fracture energy at which a single particle fails, which reveals an intrinsic length scale in the form of the mean grain size of the initial assembly. Macroscopic yield pressure is then connected with both grain size and the specific fracture process developing at the grain-scale. The impacts on macroscopic yield pressure of various grain fracture mechanisms are explored, discussed and assessed against a wide set of data at both particle and assembly scale. This work provides a new theoretical basis to estimate the effect of widely variable particle sizes in large-scale applications for which direct testing is not feasible, such as rockfill engineering and mining technologies.

[1] Northwestern University, Department of Civil and Environmental Engineering, Evanston, IL, USA

[2] The University of Sydney, School of Civil Engineering, Sydney, Australia

Accepted Manuscript

INTRODUCTION

Grain crushing is a major phenomenon controlling the performance of various geotechnical problems such as pile driving (Yang et al., 2010), dam engineering (Alonso et al., 2005), and energy production (Montgomery and Steanson, 1985). The interactions associated with distributed grain crushing cause complex deformation patterns at all scales, ranging from samples tested under laboratory conditions (Nakata et al., 2001; Lade et al., 1996), to soil-structure interaction problems involving high-stresses in soils near foundations (Zhang et al., 2012). Even more formidable challenges are encountered when the system under study involves a wide range of grain sizes, such as in rockfill dams and mining technologies (Alonso et al., 2012; Ovalle et al., 2014; Guimaraes et al., 2007). In these circumstances, the particles that constitute a large-scale prototype can be of the order of decimetres or even meters, making it impractical to test directly a representative volume of material. As a result, design procedures for these applications have to rely on properties measured from reduced model systems, with two major technical implications: (i) the effect of size-dependent grain properties is invariably lost, and (ii) rational methods are required to extrapolate the measurements from small-scale models to realistic particle geometries and stress conditions.

The solution of such problem passes necessarily from the physics controlling collective particle interactions in crushable systems. As a result, the quantification of the properties of a granular continuum can benefit from upscaling techniques able to account for grain-scale characteristics (e.g., mean grain size and grain mineralogy). Indeed, grain-scale phenomena are able to impact the constitutive properties of a granular soil, such as yield pressure, plastic compressibility, and frictional resistance (McDowell and Bolton, 1998; Coop et al., 2004; Brzesowsky et al., 2014). For this reason, various authors have linked the collective

Accepted Manuscript

crushing of sand with the fracture properties of single grains obtained from diametrical compression tests (McDowell and Amon, 2000; Nakata et al., 1999; Nakata et al., 2001). Evidences from these studies suggest that the particle strength depends considerably on factors such as size, shape and mineralogy. To capture its size-dependence, useful tools have been provided by probabilistic methods such as the Weibull's weakest link theory (Weibull, 1951, Mogi, 1962) as well as by deterministic fracture theories (Zhang et al., 1990; Brzesowsky et al., 2011; Oldecop and Alonso, 2007).

While these theories provide a first order-approximation of the size effects observed in single particle strength, their direct application becomes problematic if the response of an entire assembly is considered in a continuum mechanics context. In this case, in addition to single particle properties, other mechanisms associated with the collective response of a granular continuum must be taken into account, such as the dynamics of force chains, the rearrangement of fragments and intact grains, and the energy redistribution in the medium due to breakage (Rothenburg and Bathurst, 1989; Nguyen and Einav, 2009; Russell and Einav, 2013). It is thus readily apparent that the comminution of granular soils is affected by processes that operate at different length scales, and thus specific upscaling criteria must be established to bridge grain-scale phenomena and continuum-scale processes.

This paper is inspired by such considerations, and aims to relate the size-dependence of the fracture strength of single grains to the yield pressure of a sample made of particles with the same characteristics. For this purpose, we propose an energy scaling criterion to relate the energy input required to fracture a particle of a given diameter (Tavares and King, 1998; Yashima et al., 1987) with the work input associated with the collective crushing of grains embedded in a soil matrix (Einav, 2007a,b). In the following, an

Accepted Manuscript

analogy is established between fracture theories routinely used to tackle size-dependent failures in brittle solids and the breakage mechanics theory, which was originally conceived to model the collective crushing of brittle granular materials by modelling such solids as equivalent continua. This analogy is used together with an energy-scaling law bridging the mechanics of size-dependent fracture at particle scale with the macroscopic yielding of a granular assembly. Analytical expressions for the energy threshold associated with the brittle failure of single particles have been derived with reference to various grain-fracture models. Such models have been used to connect micro- and macro-scale phenomena through energy arguments; their predictive performances have then been assessed by comparing the model predictions with experimental data available at both scales.

ANALOGY BETWEEN FRACTURE AND BREAKAGE MECHANICS

A rational interpretation of the brittle failure of single particles can be obtained by using elastic Fracture Mechanics based on energy arguments (Griffith, 1921). According to this approach, the balance between the increment of elastic energy that is released upon the growth of a flaw and the energy that is consumed for the creation of an incremental new surface area implies that the tensile strength of a brittle solid is not only a function of intrinsic material properties, but it also depends on geometrical factors, such as the size of its internal flaws. For example, the tensile strength σ_{tc} of an infinite plate with a pre-existing elliptical crack can be expressed as follows:

$$\sigma_{tc} = \sqrt{\frac{EG_{IC}}{\pi a}} \tag{1}$$

Accepted Manuscript

where E and G_{IC} are the Young's modulus and the critical energy release rate, respectively, while a is half the length of the crack. The size dependence of the tensile strength of single grains can therefore be explained using fracture mechanics by assuming the proportionality between the crack size and the grain size (i.e., $a \propto d_p$; Zhang et al., 1990; Brzesowsky et al., 2011).

At the scale of a granular assembly, such fracture events tend to originate complex deformation processes. The Breakage Mechanics theory (Einav, 2007a) provides a conceptual basis to describe such processes in granular continua, by representing the mechanical implications of distributed grain crushing events in a homogenized way. An important feature of this theory is its ability to account for the current grain size distribution (GSD) (as well as its alterations) by defining the total Helmholtz free energy potential, Ψ, through a statistical homogenization technique:

$$\Psi\left(\boldsymbol{\varepsilon}^{\mathrm{e}}, B\right) = \left(1 - \vartheta_M B\right)\psi_r\left(\boldsymbol{\varepsilon}^{\mathrm{e}}\right) \tag{2}$$

where $\boldsymbol{\varepsilon}^{\mathrm{e}}$ is the elastic strain tensor; $0 \leq B < 1$ is the breakage, i.e. a state variable representing the relative position of the current GSD with respect to two limit states (i.e., initial GSD and ultimate GSD at complete breakage); ψ_r is the specific grainsize elastic potential for the reference grainsize; ϑ_M is a dimensionless grading index emerging from the homogenization process (Einav, 2007a).

The use of a GSD-dependent energy potential enables the description of comminution as a process involving the release of the elastic energy stored in the granular continuum and its dissipation for the alteration of the GSD (i.e., for the fracture of the grains, the creation of new surfaces and the internal redistribution of the contact forces). As a consequence, the theory of Breakage Mechanics offers a conceptual analogy with the energetics of Fracture Mechanics. Such analogy becomes even more apparent

Accepted Manuscript

if Equation (2) is connected with a dissipation potential (Einav, 2007a) to derive an energy-based yielding criterion associated with the onset of collective comminution. Under isotropic compression conditions, this process yields the following relation:

$$E_B \le \frac{E_c}{(1-B)^2} \tag{3}$$

where $E_B = -\partial\Psi/\partial B$ is the breakage energy (i.e., the 'energy release rate' due to an infinitesimal change of GSD) and E_c is the critical breakage energy (i.e. an energy threshold representing the crushability of the assembly. The latter threshold came about as an integration constant of the energy-dissipation differential equation representing the process yield (Einav, 2007c). Considering a simple linear elastic strain energy potential, it is possible to derive from (3) the expression of the comminution pressure at first yielding (i.e., B=0) under isotropic compression conditions:

$$p_{cr} = \sqrt{\frac{2KE_c}{\vartheta_M}} \tag{4}$$

where K is the bulk modulus of the granular assembly. The crushing mechanisms described at different scales by equations (1) and (4) share numerous similarities. Such similarities derive from the fact that the theories used to obtain them are both rooted on the energetics of surface area creation (Einav, 2007c). In particular, as in classic fracture theories, equation (4) involves contributions from material properties and geometric factors. For example, the effect of the stiffness properties is included in the bulk modulus K (thus suggesting that stiff particles and/or dense packing generate large yield pressures), while the role of the particle grading is embedded in ϑ_M (which tends to zero as the initial GSD approaches its ultimate configuration, thus suggesting that initially well-graded soils tend to have higher yielding thresholds

Accepted Manuscript

compared to poorly-graded soils). The picture is completed by the critical breakage energy E_c (i.e. a parameter that reflects the crushability of the material), thus playing a role conceptually similar to that of the critical energy release rate, G_{IC}.

A complete analogy would imply the treatment of E_c as a material constant, i.e. as a property that does not depend on the initial size of the particles (a factor that, based on the arguments discussed above, should instead be embedded in ϑ_M). However, unlike the dimension of length of a in equation (1), ϑ_M in equation (4) is dimensionless, since it describes the effect of the shape of the GSD, rather than its connection to absolute grain size. Indeed, recent studies on the compression response of quartz sands loaded in the crushing regime have shown that E_c displays a considerable dependence on the median grain size of the initial assembly (Fig. 1) (Zhang and Buscarnera, 2014). This finding points out the lack of an inherent length scale connected with the geometry of the particles prior to crushing and thus shows that, at variance with the critical energy release rate G_{IC}, E_c cannot be treated as an actual material property.

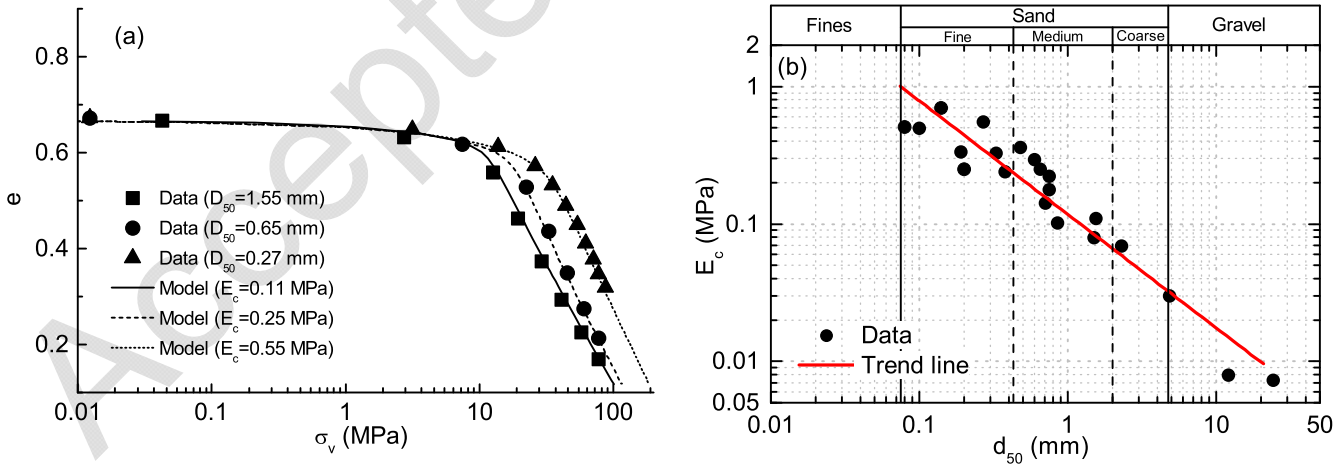

Fig. 1: a) Calibrations of E_c based on 1D compression data on silica sand samples with different mean grain sizes (data from Nakata et al., 2001) and b) summary of the calibrated E_c values over a wide range of quartz-based sand samples (Zhang and Buscarnera, 2014).

Accepted Manuscript

The goal of this study is therefore to further explore the connection between particle-scale fracture and collective crushing in grain assemblies, with the purpose to establish a stronger connection between the two above-mentioned mechanical theories. Fulfilment of such task will offer a fundamental insight on the connection between macroscopic comminution and yielding and particle properties such as mineralogy, intrinsic fracture constants (e.g., G_{IC}) and basic grain-scale characteristics (e.g., grain size and shape).

BRIDGING GRAIN-SCALE FRACTURE AND COLLECTIVE BREAKAGE

To explain the grainsize dependence of the energy threshold associated with collective particle breakage, it is necessary to study the micromechanics of grain crushing. For this purpose, let us consider the energy input required to crush a single grain. This quantity can be measured through uniaxial compression tests (Fig. 2), following an approach often used to characterize the grindability of granular materials as a function of their size (Yashima et al., 1987; Ryu and Saito, 1991; Tavares and King, 1998). In particular, a specific value of fracture energy per unit volume, E_{pc}, can be calculated as follows:

$$E_{pc} = \frac{1}{V_p}\int_0^{\Delta_f} F d\Delta \qquad (5)$$

Where F is the applied load during the test, Δ_f is the displacement once particle failure occurs, and V_p is the volume of the particle (assumed constant during the test). Experiments on brittle grains suggest that E_{pc} is a size-dependent quantity well approximated by a power law of the form $E_{pc} \propto d_p^{-\lambda}$ (Yashima et al., 1987).

Accepted Manuscript

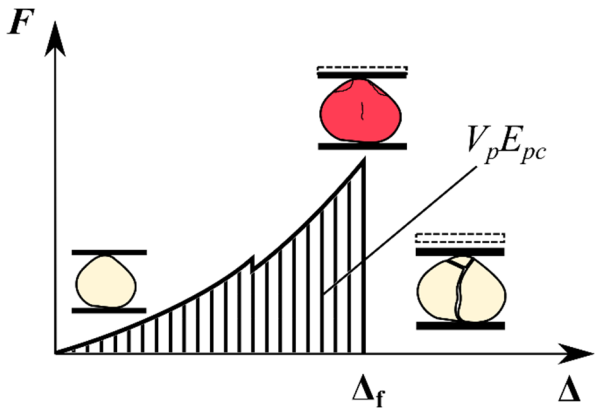

Fig. 2: Schematics of diametrical compression of a single grain. The area under the force-displacement curve represents the energy threshold at the onset of fracture (V_pE_{pc}). The red colour indicates the achievement of critical energy content at which the particle fractures catastrophically under the imposed conditions.

Next, consider the process of energy storage and consequent fracture for particles embedded in a soil matrix subjected to an isotropic state of stress (Fig. 3a). Prior to comminution, brittle particles in a densely packed granular system tend to undergo a first stage of nearly reversible compaction that can be well approximated as an elastic process. During this stage the particles store elastic energy through deformations at the inter-granular contacts. When the elastic stored energy in a sufficient number of grains exceeds the local threshold E_{pc}, crushing occurs in a distributed manner. This is followed by the dissipation of energy through the creation of new surfaces, the internal re-distribution of contact forces and the accumulation of permanent compaction. This process continues until a force network able to sustain the macroscopic state of stress is formed, with the new configuration characterized by the presence of smaller particles with larger crushing resistance (i.e., with higher values of E_{pc}). The accumulation of these events manifests macroscopically in the form of plastic yielding (i.e. the sharp increase in the compressibility of the specimen) and through the ability to sustain larger compressive stresses (often referred to as clastic hardening; McDowell et al., 1996).

Accepted Manuscript

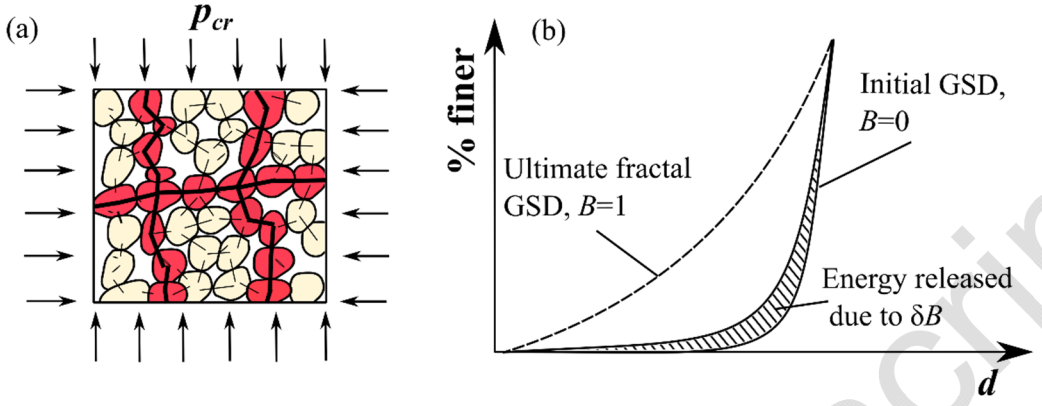

Fig. 3: Schematics of isotropic compression test and graphical interpretation of the critical breakage energy E_c

In the breakage mechanics theory, E_c controls the value of the work input at which the elastic energy stored in the particles can be released collectively by causing an infinitesimal shift of the initial GSD (δB, as reflected by the shaded area in Fig. 3b). To bridge processes at particle and assembly scales we propose a linear relationship between E_c and E_{pc} as follows:

$$E_c = (1-n)\xi E_{pc} \tag{6}$$

where n is the packing porosity and ξ is a scaling factor. The term (1-n) is included to transform the single-grain fracture energy threshold E_{pc}, defined per unit volume of solid, to the critical breakage energy, E_c, defined per unit volume of the granular continuum. The scaling in (6) can also be written in terms of elastic stored energy. In particular, by combining equations (2) and (3), the onset of comminution (i.e. B = 0) at specimen scale can be characterized by:

$$\Psi(\boldsymbol{\varepsilon}^{\mathrm{e}}) \le \frac{E_c}{\vartheta_M} \tag{7}$$

Accepted Manuscript

By analogy, the criterion for the onset of grain fracture can be expressed in terms of elastic energy stored in the particle, Ψ_p:

$$\Psi_p(\Delta) \leq E_{pc} \tag{8}$$

Equation (6) imposes therefore a proportionality condition between the energy stored in the solid volume at the triggering of crushing at the two considered length scales:

$$\Psi(\boldsymbol{\varepsilon}^{e}_{cr}) = \frac{(1-n)\xi}{\vartheta_M}\Psi_p(\Delta_f) \tag{9}$$

where $\boldsymbol{\varepsilon}^{e}_{cr}$ is the elastic strain at onset of comminution. Based on equation (9), the scaling factor ξ may be interpreted as a function of the ratio between strain energy density averaged across the volume of a soil matrix at the verge of collective comminution and the same quantity of individual particles at the verge of fracture. While this interpretation can in principle be assessed through the direct quantification of ξ via numerical techniques (e.g., DEM analyses), it is possible to show that the value of ξ in (9) does not affect the size effects predicted at particle and/or assembly scale. As a result, since the aim of this paper is to provide a mechanistic interpretation of grainsize dependencies through fracture and breakage principles, the detailed analysis of ξ is considered to be outside the scope of this work, and this property will simply be treated as a constant to be evaluated on the basis of available evidences.

The hypothesis summarized by equation (6) will be used in the following to incorporate into macroscopic yielding conditions the role of some fundamental properties of the constituting particles (e.g., their size, d_p, critical energy release rate, G_{IC}, and elastic constants, E and v). For this purpose, the first step is to use specific micro-scale fracture models to study in detail the energetics of fracture in single grains (i.e., E_{pc}).

Accepted Manuscript

ENERGY STORAGE AT PARTICLE SCALE

Assuming that the grains are made of linear elastic material, the load-displacement behaviour of an idealized contact between a grain and a rigid plate can be described through different types of elastic contact models. The force-displacement relation at inter-granular contacts has been modelled using three simple geometrical schemes (i.e., flat, spherical, and conical contacts as shown in Fig. 4).

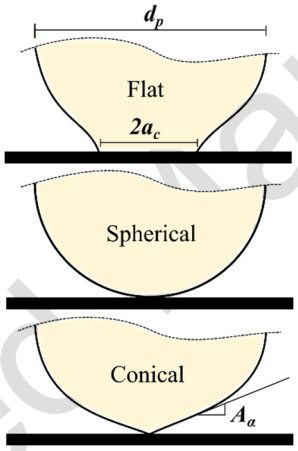

Fig. 4: Schematics of different contact elasticity models

A flat contact can be assumed to have constant contact area as the load increases. Thus, it can be described via a linear relation, as follows:

$$F = \frac{E\pi a_c^{\,2}}{R}\delta \tag{10}$$

where a_c is the contact radius; R the particle radius; and δ the contact deformation. The contact between an elastic sphere and a rigid plate is a particular case of the Hertzian solution for two contacting elastic spheres

Accepted manuscript

(Timoshenko and Goodier, 1951). Such a solution is recovered when both the radius and the stiffness of the second sphere tend to infinity:

$$F = \frac{4}{3} R^{\frac{1}{2}} \left(\frac{1-\nu^2}{E} \right)^{-1} \delta^{\frac{3}{2}} \quad \text{with} \quad a_c = \sqrt{R\delta} \tag{11}$$

where ν is the Poisson's ratio. In this case the contact radius a_c grows upon increasing values of contact forces. The nonlinear load-deformation responses of conical contacts has been studied first by Goddard (1990) to explain the pressure-dependence of elastic wave velocity in granular materials. Jäger (1999) has later provided a more general solution from which it is possible to recover the linear, Hertzian and conical contact models as particular cases. Using this solution, the load-deformation response of a conical contact is given by:

$$F = \frac{E}{1-\nu^2} \left(\frac{2}{\pi A_s} \right)^{\frac{1}{2}} \delta^2 \quad \text{with} \quad a_c = \frac{2}{\pi A_s} \delta \tag{12}$$

where A_s represents the tangent of the inclination angle of the conical surface with respect to the plate (see Fig. 4).

BRITTLE FAILURE AT PARTICLE SCALE

The fracture resistance of individual particles is often quantified via the characteristic strength σ_{pc}, which is typically measured through diametrical compression tests between two plates (Jaeger, 1967):

$$\sigma_{pc} = \frac{F_f}{d_p^2} \tag{13}$$

where F_f is the failure load and $d_p = 2R$ is the particle diameter. It is worth noting that the characteristic strength (13) is related to the tensile strength of the material but it does not necessary coincide with it.

Accepted Manuscript

Elastic analyses of diametrically loaded spheres indicate that the largest tensile stress is located at the centre of the particle along the median axis (Hiramatsu and Oka, 1966). These results suggest that particle crushing occurs because of tensile failure inside the sphere, and have been widely used to back-calculate the tensile strength of brittle particles (Yashima et al., 1987; Tavares and King, 1998). Shipway and Hutchings (1993) argued that this conclusion is valid only up to a certain level of contact deformation (i.e., up to when $a_c/R \approx 0.6$), beyond which the tensile stresses at the surface become larger than the tensile stress along the median axis. This has led to the hypothesis that particles may fail because of the propagation of surface flaws rather than body cracks, which has been used for Hertzian fracture models of grain contacts (Zhang et al., 1990; Brzesowsky et al., 2011). Experiments on glass beads performed by Salman and Gorham (2000) have shown that cracks may first nucleate at the contact, then propagating along the median plane, to finally cause failure of the whole particle through central splitting. Since it is arguable that both contact and centre cracks contribute to grain fracturing, here we explore in parallel both possibilities, deriving failure models for both volume and surface cracks. In particular, two scenarios are considered: (i) penny-shaped cracks located at the centre of the particle; and (ii) edge cracks oriented perpendicularly to the maximum hoop tensile stress at the contact surface.

In addition to these deterministic models of grain fracturing (both based on linear elastic solutions), a statistical interpretation based on the Weibull's weakest link theory of randomly distributed volume cracks will be considered as a further criterion to explain the size-dependence of the particle strength. It is also possible to assume randomly distributed surface cracks for Weibull's interpretation that gives slightly different model parameters (Lim et al., 2004; McDowell and de Bono, 2013). For the sake of simplicity,

Accepted Manuscript

however, here the probabilistic interpretation based on Weibull's statistics will be limited only to the standard case of flaws distributed within the bulk volume.

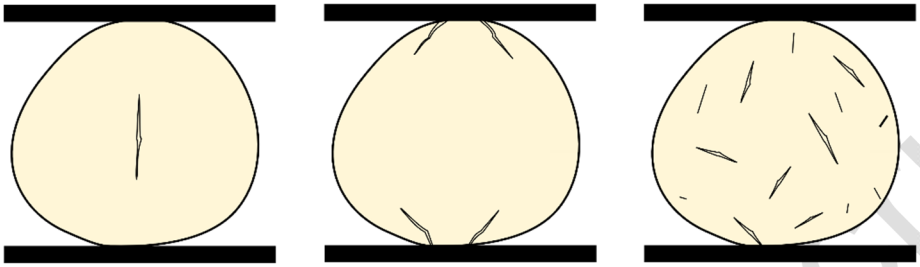

Fig. 5: Schematics of different failure models: a) centre crack; b) contact crack and c) random crack

Centre crack

The tensile stress along the median axis can be approximated by using the following relation (Hiramatsu and Oka, 1966):

$$\sigma_t = \frac{2.8F}{\pi d_p^{\,2}} \tag{14}$$

The stress intensity factor corresponding to a penny shaped crack (Kassir and Sih, 1966) is given by:

$$K_I = \frac{2}{\sqrt{\pi}}\sigma_t\sqrt{a} \tag{15}$$

where a is the crack radius. The crack will propagate when K_I coincides with the fracture toughness for mode I, K_{IC}. Considering the Irwin's relation linking K_{IC} to critical energy release rate G_{IC} and elastic properties (E, ν), it is possible to express the tensile stress at crack extension as follows:

$$\sigma_{tc} = \frac{\sqrt{\pi}}{2\sqrt{a}}\sqrt{\frac{G_{IC}E}{1-\nu^2}} \tag{16}$$

Accepted Manuscript

Assuming that the crack size scales linearly with the grain size (i.e., $a = \alpha R$, α being a dimensionless factor), it is possible to recover a size-dependence law for the tensile strength:

$$\sigma_{tc} = \frac{\sqrt{\pi}}{\sqrt{2\alpha}} \sqrt{\frac{G_{IC}E}{1-\nu^2}} d_p^{-\frac{1}{2}} = a' \sqrt{\frac{G_{IC}E}{1-\nu^2}} d_p^{-\frac{1}{2}} \tag{17}$$

where a' is a coefficient associated with the geometry of the problem. The load at crack extension can be obtained by equating the critical stress (17) to the maximum tensile stress along the median axis (14):

$$F_f = \frac{\pi a'}{2.8} \sqrt{\frac{G_{IC}E}{1-\nu^2}} d_p^{\frac{3}{2}} \tag{18}$$

Contact crack

The tensile stress around a Hertzian contact is maximized at the edge of the contact zone (Timoshenko and Goodier, 1951):

$$\sigma_t = \frac{1-2\nu}{2} \frac{F}{\pi a_c^2} \tag{19}$$

A crack with size $a \propto d_p$ aligned along the hoop of the Hertzian contact and perpendicular to the tensile stress field can be approximated as an edge crack in a semi-infinite medium (Frank and Lawn, 1967; Zhang et al., 1990). Its stress intensity factor is given by:

$$K_I = 1.12 \sigma_t \sqrt{\pi a} \tag{20}$$

Assuming that $K_I = K_{IC}$ at the onset of fracture, the critical tensile stress for crack extension can be expressed as:

$$\sigma_{tc} = \frac{1}{1.12} \left(\frac{\pi\alpha}{2} \right)^{-\frac{1}{2}} \sqrt{\frac{G_{IC}E}{1-\nu^2}} d_p^{-\frac{1}{2}} = b' \sqrt{\frac{G_{IC}E}{1-\nu^2}} d_p^{-\frac{1}{2}} \tag{21}$$

Accepted Manuscript

where b' is another coefficient associated with the geometry of the problem. The failure load due to contact crack is given by equating (19) with (21):

$$F_f = \frac{9}{64}\left(\frac{2\pi b'}{1-2\nu}\right)^3 \left(\frac{1-\nu^2}{E}\right)^{\frac{1}{2}} G_{IC}^{\frac{3}{2}} d_p^{\frac{1}{2}} \tag{22}$$

Weibull's statistics

An alternative way to capture the size-dependence of the particle strength is to interpret it in statistical rather than deterministic manner. A common strategy is to use the Weibull's weakest link theory to describe the survival probability P_s of a batch of particles subjected to a given stress σ_{pc} (Nakata et al., 1999):

$$P_s\left(\sigma_{pc}, V_p\right) = \exp\left[-\frac{V_p}{V_{p0}}\left(\frac{\sigma_{pc}}{\sigma_{pc,0}}\right)^w\right] \tag{23}$$

where V_p is the particle volume; $\sigma_{pc,0}$ is the characteristic stress at which 37% of the particles of volume V_{p0} survive; $w>0$ is the Weibull modulus, i.e. a constant that reflects the variability of the particle strength. Equation (23) implies that the σ_{pc} corresponding to a selected survival probability is a function of the particle size, as follows (Mogi, 1962):

$$\sigma_{pc} = \sigma_{pc,0}\left(\frac{d_p}{d_{p0}}\right)^{-\frac{3}{w}} \tag{24}$$

where d_{p0} is the reference particle size corresponding to particle volume V_{p0}. Using equation (13), it is possible to express the failure load as follows:

$$F_f = \sigma_{pc,0} d_{p0}^{\frac{3}{w}} d_p^{2-\frac{3}{w}} \tag{25}$$

Accepted Manuscript

Equations (18), (22) and (25) provide analytical expressions of the failure load of diametrically loaded particles, and predict different degrees of size dependence (i.e., $\sigma_{pc} \propto d_p^{-\eta}$), which for the three considered cases of centre crack, contact crack and random volume cracks correspond to power-law coefficients η = 0.5, 1.5 and (3/w), respectively.

SPECIFIC FRACTURE ENERGY AT PARTICLE SCALE

By combining elastic and failure models it is possible to derive the fracture energy per unit volume at the onset of particle failure. For this purpose, the particle diameter d_p of non-spherical grains corresponds to its volume-equivalent sphere (hereafter adopted as a measure of particle size). The specific fracture energy E_{pc} corresponding to different elastic models can be linked to the particle characteristic strength σ_{pc} by substituting equations (10-12) into (5). Noting that a uniaxially loaded particle has two contacts, the particle axial deformation Δ is twice the deformation of a particle-plate contact deformation δ under similar load F (i.e. $\Delta(F)=2\delta(F)$). Integration of equation (5) leads to:

Linear contact:
$$E_{pc} = \frac{12}{E\pi^2}\left(\frac{a_c}{R}\right)^{-2}{\sigma_{pc}}^2 \tag{26}$$

Hertzian contact:
$$E_{pc} = 4.989\frac{1}{\pi}\left(\frac{1-\nu^2}{E}\right)^{\frac{2}{3}}{\sigma_{pc}}^{\frac{5}{3}} \tag{27}$$

Conical contact:
$$E_{pc} = 3.360 A_s^{\frac{1}{4}}\pi^{-\frac{3}{4}}\left(\frac{1-\nu^2}{E}\right)^{\frac{1}{2}}{\sigma_{pc}}^{\frac{3}{2}} \tag{28}$$

The characteristic strength σ_{pc} in (26)-(28) can be further expressed in terms of grain size by combining Equations (18), (22) and (25) with (13). While the failure criteria based on centre cracks and Weibull's statistics can be combined with any of the three elastic models, the failure criterion for contact cracks can

Accepted Manuscript

only be used in combination with the Hertzian contact theory, on the basis of which it was explicitly derived. As a result, seven expressions of E_{pc} are obtained:

A. Failure at centre cracks:

I) Linear contact $$E_{pc} = 1.532 a'^{2} \frac{G_{IC}}{1-\nu^2}\left(\frac{a_c}{R}\right)^{-2} d_p^{-1} \quad (29)$$

II) Hertzian contact $$E_{pc} = 0.897 \pi^{\frac{2}{3}} a'^{\frac{5}{3}} \left(\frac{1-\nu^2}{E}\right)^{-\frac{1}{6}} G_{IC}^{\frac{5}{6}} d_p^{-\frac{5}{6}} \quad (30)$$

III) Conical contact $$E_{pc} = 0.717 \pi^{\frac{3}{4}} a'^{\frac{3}{2}} A_\alpha^{\frac{1}{4}} \left(\frac{1-\nu^2}{E}\right)^{-\frac{1}{4}} G_{IC}^{\frac{3}{4}} d_p^{-\frac{3}{4}} \quad (31)$$

B. Failure at contact cracks:

I) Hertzian contact $$E_{pc} = 6.071 \pi^{-1} b'^{5} \left(\frac{\pi}{1-2\nu}\right)^{5} \left(\frac{1-\nu^2}{E}\right)^{\frac{3}{2}} G_{IC}^{\frac{5}{2}} d_p^{-\frac{5}{2}} \quad (32)$$

C. Failure of weakest link (Weibull's statistics):

I) Linear contact $$E_{pc} = 12 \pi^{-2} \left(\frac{a_c}{R}\right)^{-2} \frac{1}{E} \sigma_{pc,0}^{2} d_{p0}^{\frac{6}{w}} d_p^{\frac{-6}{w}} \quad (33)$$

II) Hertzian contact $$E_{pc} = 4.989 \pi^{-1} \left(\frac{1-\nu^2}{E}\right)^{\frac{2}{3}} \sigma_{pc,0}^{\frac{5}{3}} d_0^{\frac{5}{w}} d_p^{\frac{-5}{w}} \quad (34)$$

III) Conical contact $$E_{pc} = 3.360 \pi^{-\frac{3}{4}} A_\alpha^{\frac{1}{4}} \left(\frac{1-\nu^2}{E}\right)^{\frac{1}{2}} \sigma_{pc,0}^{\frac{3}{2}} d_0^{\frac{9}{2w}} d_p^{\frac{-9}{2w}} \quad (35)$$

Table 1 assembles the power law coefficients that reflect the size dependence of the particle fracture energy according to the seven analytical models discussed above.

Table 1: Grainsize effect on the fracture energy per unit volume of solid, in terms of the power law coefficient λ

$E_{pc} \propto d_p^{-\lambda}$	Centre crack	Contact crack	Weibull's statistics
Linear elasticity	1	N/A	6/*w*

Accepted Manuscript

Hertzian elasticity	0.833	2.5	5/*w*
Conical elasticity	0.75	N/A	4.5/*w*

ENERGY STORAGE AND CLASTIC YIELDING AT SPECIMEN SCALE

Various options are available to model the mechanism of energy storage in granular soils. Some of these options have been documented in detail by Einav (2007b) and Nguyen and Einav (2009). Here, the following pressure-dependent elastic energy potential is used in conjunction with equation (2) to guarantee versatility and good agreement with experimental data for granular materials:

$$\psi_r\left(\boldsymbol{\varepsilon}^{\mathrm{e}}\right)=\frac{p_r}{\bar{K}\left(2-m\right)}\Lambda_v^{\frac{2-m}{1-m}}+\frac{3}{2}p_r\bar{G}\Lambda_v^{\frac{m}{1-m}}\varepsilon_s^{\mathrm{e}2} \tag{36}$$

where $\Lambda_v=\bar{K}\left(1-m\right)\varepsilon_v^{\mathrm{e}}+1$; p_r is a reference pressure usually taken as 1 kPa; $\bar{K}$ and $\bar{G}$ are non-dimensional elastic constants, and *m* describes the pressure dependence of the macroscopic elastic stiffness. In particular, *m* = 0 implies linear elasticity (i.e., no pressure dependence), *m* = 1/3 a pressure-dependence typical of Hertzian contacts and *m* = 1/2 a pressure-dependence typical of conical contacts (Goddard, 1990). For general triaxial loading, the breakage yield criterion (3) must be enriched by considering the energy stored in the form of elastic shear strains, as well as frictional dissipation (Einav, 2007b):

$$\frac{E_B}{E_c}\left(1-B\right)^2+\left(\frac{q}{Mp}\right)^2-1\le 0 \tag{37}$$

where *M* is the stress ratio at frictional failure; *p* and *q* are mean and deviatoric stresses. Typical simulation results for 1D compression tests based on equations (36) and (37) are illustrated in Fig. 6, where the post-yielding behaviour is captured through the coupling angle parameter (ω) that relates the rate of volumetric plastic dissipation and the rate of breakage dissipation (Einav, 2007b; Nguyen and Einav, 2009). One can

Accepted Manuscript

see that larger values of E_c imply the growth of the elastic domain, thus increasing the predicted yield pressure.

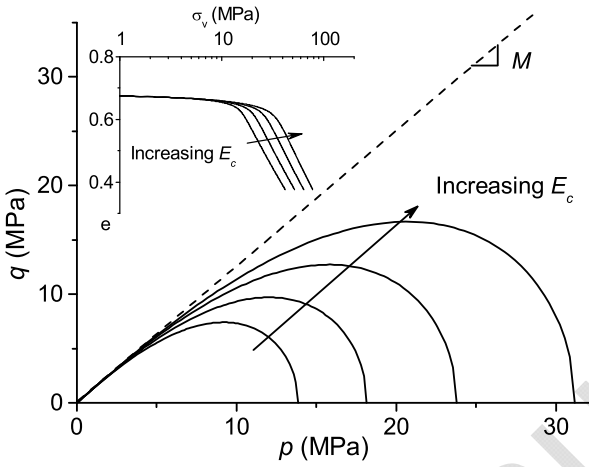

Fig. 6: Typical yield surfaces and 1D compression response for different values of E_c.

PARAMETER CALIBRATION AND ASSESSMENT OF MODEL PERFORMANCE

Analyses at particle scale

The three analytical failure models corresponding to the different scenarios of pre-existing crack geometry are here calibrated against two sets of data. The first dataset reported by Nakata et al. (2001) involves single particle tests performed on three batches of Silica sand grains and one batch of Toyoura sand grains of different sizes (Fig. 7a). The second dataset reported by McDowell (2002) includes survival probability curves for three batches of Leighton Buzzard sand of varying grain size; such curves have been used to compute the mean particle strength values, $\bar{\sigma}_{pc}$, reported in Fig. 7b.

The parameters of each particle scale model have been calibrated on the basis of reported evidences. For the statistical failure model, the Weibull modulus w has been set to be equal to the reported values calibrated

Accepted Manuscript

from survival probability tests. Similarly, the mean strength $\bar{\sigma}_{pc,0}$ for a given particle size d_{p0} has been chosen in accordance with the reported probability distributions. For the two deterministic failure models, the Young's modulus E and the Poisson's ratio v have been set to 95.6 GPa and 0.077, respectively, while the critical energy release rate G_{IC} has been set to 0.95 J/m^2 (corresponding to K_{IC} = 0.31 MPa/m$^{0.5}$), in accordance with values reported by Zhang et al. (1990) for quartz. Since the geometric factors a' and b' do not influence the predicted size-effect, their values have been selected to obtain a best match of the average strength for an arbitrarily selected grain size (i.e. d_{p0} = 2mm). Therefore, by anchoring the size effect curves on the same point in the σ_{pc} - d_p plane, this choice enables a straightforward graphical comparison of the predictions provided by the three failure modes (see Fig. 7). The calibrated parameters based on the two datasets are listed in Table 2. Since the two considered sands have similar mineralogy (> 99% quartz) and grain geometry (rounded grains), the corresponding parameters are very similar. For the sake of brevity, the following analyses have been performed only by using the parameters calibrated for Leighton Buzzard sand.

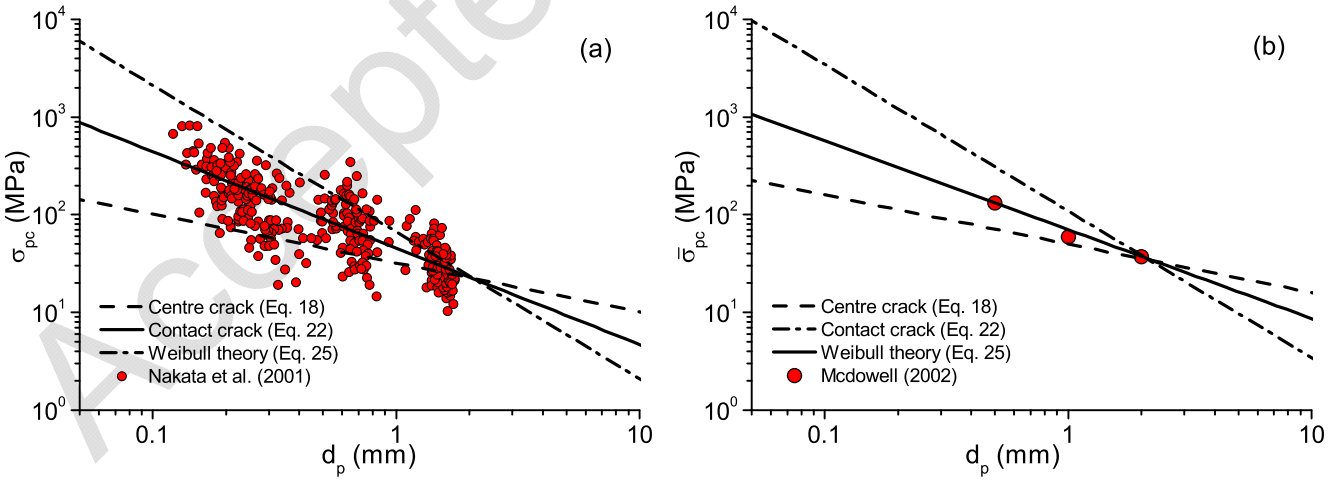

Fig. 7: a) Predicted grain size effect for three batches of Silica with grain size range (0.25-0.3)mm, (0.6-0.71)mm and (1.4-1.7)mm and one batch of Toyoura sand with grain size range (0.11-0.25)mm (data from Nakata et al. (2001)); b) Predicted grain size effect of the average characteristic strength of Leighton Buzzard sand grains (data from McDowell (2002)).

Accepted Manuscript

Table 2: Calibrated parameters based on particle strength datasets

	Nakata et al. (2001)	McDowell (2002)
E (GPa)	95.6	95.6
v	0.077	0.077
G_{IC} (J/m^2)	0.95	0.95
a'	3.0	4.7
b'	230	271
w	3.04	3.3
$\bar{\sigma}_{pc,0}$ (MPa)	23	37.5
d_{p0} (mm)	2	2

The slope of the trend lines reported in the figure is related only to the assumed failure mechanisms. As a result, the predicted size effect can be used to validate the accuracy of the various particle-scale hypotheses against evidences of size-dependent strength. Note that the slope of trend line predicted by the Weibull's theory based on a value of w calibrated from the available particle strength statistics gives the best agreement with the trends observed on both Silica/Toyoura and Leighton Buzzard sands (i.e., slope of –1). On the other hand, the trend lines predicted by the centre and contact crack models provide a lower and upper bound of size effect, respectively (i.e., slopes of -0.5 and -1.5). Fig. 7 shows that such predicted values bound reasonably well the data scatter observed in the tests. A possible explanation for this result is that particles from the same batch may not necessarily undergo the same type of failure. In other words, measured values of particle strength can be an outcome of different failure patterns affected by varying

Accepted Manuscript

size/location of the flaws, particle angularity, and orientation of the applied forces. As a result, the analytical solutions based on the hypothesis of pre-existing centre and/or contact cracks can be seen as two particular cases among all the possible strategies to inspect the size dependence of the particle strength. Given the inherent complexity of addressing such a multiplicity of mechanisms, the Weibull's theory is therefore a useful tool to encompass statistically different failure modes and capture the observed size-dependence of particle strength. Under this perspective, it is interesting to note that the Weibull moduli that match the slopes of the trend lines predicted by the two deterministic models with $w = 2$ for contact crack and $w = 6$ for centre crack, respectively. Such values encompass the majority of w values reported in the literature on the basis of point load tests on single particles, as summarized in Table 3. Clearly values of w that fall beyond such ranges are also possible, and can be interpreted as cases in which the two deterministic failure mechanisms considered in this work do not capture accurately the actual mode of failure taking place in those experiments.

Table 3: Summary of the reported Weibull modulus for glass beads, sands and gravels

Method	Source	Material	Size (mm)	Weibull modulus w
Calibrated from strength statistics	Nakata et al. (1999)	Quartz	1.18~1.4	4.2
	Nakata et al. (2001)	Silica	1.4~1.7	3.04
			0.6~0.71	2.17
			0.25~0.3	1.82
		Toyoura sand	0.106~0.25	2.17
		Glass beads	0.85~1.0	5.9
	McDowell (2002)	Leighton Buzzard sand	0.5	3.44
			1	2.34
			2	3.14
	McDowell and Amon (2000)	Quiou sand	1~16	1.32~1.93

Accepted Manuscript

	Lim et al. (2004)	Railway blast (25~30% quartz)	8~30	2.61~4.22
	Brzesowsky et al. (2011)	Beaujean sand	0.115~0.378	5.74~6.38
Back calculated from strength size effect	Lee (1992)	Leighton Buzzard sand	1~3	8.40
	Yashima et al. (1987)	Borosilicate glass	0.1~3	5.93
		Quartz	0.05~10	2.57~6.49

While the assumed failure mode plays a dominant role on the size dependence of the particle strength, the choice of the contact model affects the power law relationship between σ_{pc} and E_{pc} (equations (26)-(28)). In particular, linear, Hertzian and conical contact models predict slopes of 2, 1.66 and 1.5, respectively. To validate the elastic models against measurements, the predicted trend lines in the σ_{pc}-E_{pc} planes have been reported together with published data. The datasets used here are those by Yashima et al. (1987) and Tavares and King (1998) who reported σ_{pc} and E_{pc} from uniaxial crushing tests on nearly perfect spherical quartz particle and glass beads (Fig. 8). While a larger data scatter can be noticed for the case of quartz sand particles because of their natural variability, the comparison shows that the best match for both materials is offered by the hypothesis of Hertzian contact. Such finding can be interpreted as an outcome of the fact that both data sets have been obtained by using particles of nearly spherical shape. By contrast, conical contact laws can be expected to provide a better performance in case of angular particles.

Accepted Manuscript

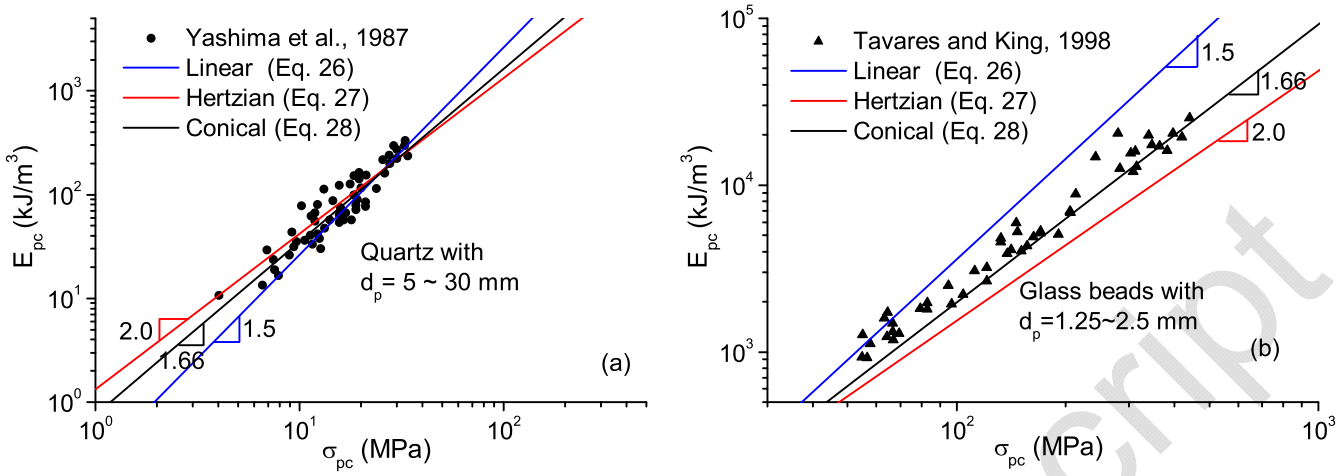

Fig. 8: Experiments vs. predictions for (a) spherical quartz grains (Yashima et al., 1987) and (b) glass beads (Tavares and King, 1998) using equations (26)-(28) on σ_{pc} - E_{pc} plane. The mass specific fracture energy originally reported in these studies were converted to volume specific one using specific gravity G_s = 2.65 for quartz and 2.25 for glass beads. The input parameters for the equations are E = 95.6 GPa and ν=0.077 for quartz and E = 70 GPa and ν=0.16 for glass beads. In both figures, the same contact shape factors a_c/R = 0.22 for linear elasticity and A_s =0.007 for conical elasticity are used for comparision purpose.

Fig. 9a reports in the E_{pc} - d_p plane the size dependence of the energy at the onset of particle fracture predicted by combining the Hertzian elastic contact with various failure models. The model predictions are compared against data on spherical quartz grains reported by Tavares and King (1998). It is found that the fracture energy model calibrated with a value of w derived from previous studies on particle strength (McDowell, 2002) provides the best match for both the magnitude and the size dependence of the measured energy data. The shaded area in the figure provides instead the scatter of the fracture energy predicted for values of Weibull modulus w varying between the two bounds associated with fracture at centre cracks and at contact cracks, i.e. associated with different potential failure mechanisms. Fig. 9b collects the seven analytical models for E_{pc} by using all the combinations of failure and contact laws discussed in this paper. It is shown that the particle failure mode plays a key role in determining the size effects, while the elastic model at the contact induces only second-order alterations of the predicted trends. Among all of these

Accepted Manuscript

models, the Weibull's theory combined with Hertzian elasticity is found to provide the best agreement with experimental data. This finding is consistent with the observations in Figs. 7 and 8, showing that the Weibull's theory and Hertzian elasticity best capture the data for rounded or sub-rounded particles reported on the σ_{pc} - d_p and E_{pc} - σ_{pc} plane, respectively.

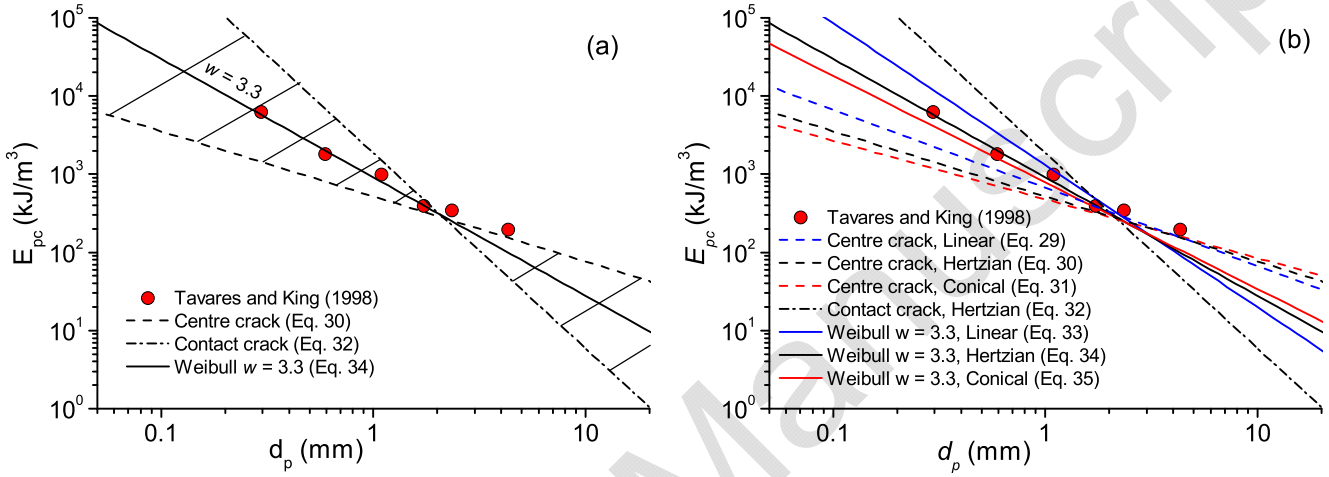

Fig. 9: Reported values of E_{pc} plotted against particle diameters for spherical quartz: a) performance of Hertzian elasticity and b) performance of the seven combinations of the elasticity models and failure modes.

Analyses at continuum scale

Results from the 1D compression of Leighton Buzzard sand (McDowell, 2002) can be used for the assessment of the performance of the proposed energy-based theory across scales. The predicted E_{pc} trend lines using its parameters (Table 2) can be upscaled into macroscopic critical breakage energy E_c through relation (6). Based on their optimal performance in capturing evidences at particle scale, Weibull-type failure and Hertzian elasticity models have been chosen for the upscaling. For each specimen, the average grain size reported by the authors has been used to evaluate the fracture energy E_{pc} of its constituting particles. This value has been then upscaled to compute the macroscopic critical breakage energy threshold

Accepted Manuscript

E_c by employing a scaling factor $\xi = 0.25$. Such value is similar to the ratio between particle strength and macroscopic yielding stress reported by McDowell (2002) for the same sand, and it is used here as a first-order hypothesis to define the ratio between the energy thresholds at the two length scales. Such hypothesis can in principle be assessed and corroborated quantitatively through direct numerical simulations (e.g., by means of DEM analyses), which are beyond the scope of this paper. Fig. 10 presents the compression response predicted by the breakage mechanics theory using the upscaled values of E_c for three specimens characterized by a different initial mean grain size. The model parameters are summarized in Table 4. The values of yielding stress, as well as their size dependence, are captured satisfactorily, thus corroborating the applicability of the proposed upscaling procedure.

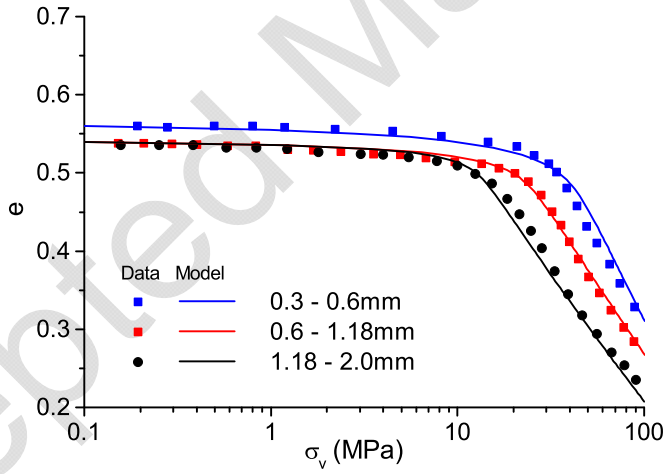

Fig. 10: Measured vs. predicted 1D compression responses of Leighton Buzzard sand (data from McDowell (2002)).

Fig. 11 reports the trend lines predicted by the theory in the E_c - d_{50} plane in comparison with the dataset reported by Zhang and Buscarnera (2014). In this case the median grain size d_{50} is approximated as the mean grain size to compute E_{pc}, and the upscaling is again performed via equation (6) with $\xi = 0.25$. It can

Accepted Manuscript

be noted that the three trend lines predicted by the theory encompass the range of variation associated with the considered data points. In this case, the grainsize dependence reflected by the dataset is found to be closer to the theoretical prediction by a centred crack failure model, while the predictions of the Weibull's theory based on parameters calibrated from the previous examples is less successful. A possible reason for this result is the much larger variability of the mineral properties and grain geometries that characterize the sands considered in the dataset. In other words, the average particle strength and Weibull modulus of the various sands are not necessarily the same as those used for Leighton Buzzard sands, thus causing a data scatter that may tend to shift from the trend line computed for w=3.3. By contrast, the values of E_c for Leighton Buzzard sands that were used for Fig. 10 (i.e., soil samples made of sand grains characterized exactly by w=3.3) tend to follow the predicted trend line associated with w=3.3 (squared symbols in Fig. 11). In addition, the range of variation reported in Fig. 11 is found to be satisfactorily bounded by the trend lines computed from the two deterministic failure modes. This result further corroborates the size effect on E_{pc} that has been predicted by combining the Hertzian elastic contact model with the three considered failure criteria, as well as the grainsize dependent relation of E_c obtained through the proposed energy upscaling law.

Table 4: Breakage mechanics parameters for 1D compression tests by McDowell (2002)

d (mm)	0.3 – 0.6	0.6 – 1.18	1.18 – 2.0
e_0	0.56	0.54	0.54
E_c (Mpa)	0.49	0.18	0.073
ϑ_M	0.7693	0.7767	0.7817
$\bar{K}$	7800	8800	8800
$\bar{G}$	4680	5280	5280
ω (°)	63.5	65	68.5
M	1.3	1.3	1.3

Accepted Manuscript

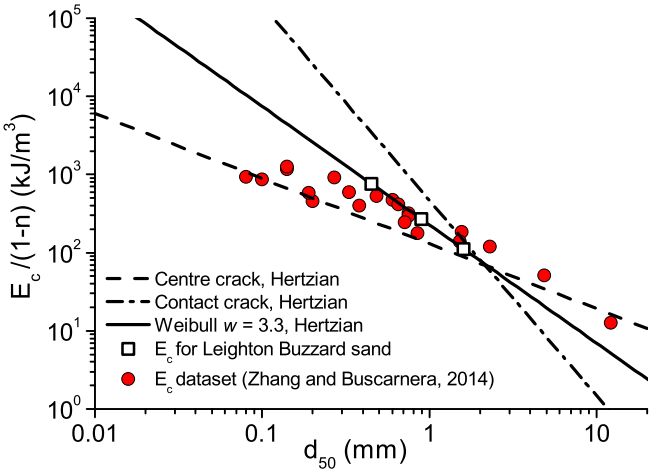

Fig. 11: Comparison of E_c dataset with three upscaled E_{pc} models via equation (6) with an upscaling factor $\xi = 0.25$.

DISCUSSION

The theoretical formulae derived in this work can be used to address a variety of technical challenges. For example, they provide theoretical support to estimate the value of macroscopic mechanical quantities for assemblies made of very large particles (i.e., granular systems for which representative specimens are not practical to be tested in a laboratory). This can be done by first measuring these properties on representative samples of soils composed by much smaller grains; then the compression properties of large-scale samples (e.g., yielding pressures and compressibility) can be estimated through a logic similar to that proposed by Frossard et al. (2012) for the shear strength of rockfill. Such a task can be pursued by combining equation (6) with one of the micro-scale models for E_{pc} (equations (29)-(35)), thus obtaining scaling relations of the type

$$E_c \propto d_{50}^{-\lambda} \tag{38}$$

Accepted Manuscript

A single point of calibration is therefore needed, which can be obtained by conducting standard compression experiments on samples of standard dimensions (i.e., considering a specific grain size to evaluate reference values of $E_{c,ref}$ and $d_{50,ref}$). In this way, equation (38) can be rewritten as:

$$E_c = E_{c,ref}\left(\frac{d_{50}}{d_{50,ref}}\right)^{-\lambda} \tag{39}$$

The power law coefficient λ in equation (39) can be estimated either by using one of the analytical models discussed in the previous sections or by measuring the Weibull modulus of the constituting particles.

Another useful application of the connection of breakage mechanics and fracture mechanics is the possibility to relate the yield pressure of a granular matrix with fundamental physical properties of the constituting minerals (e.g., elastic constants, fracture toughness or specific surface energy). For example, a centre crack model would suggest a scaling of the particle strength with $G_{IC}^{1/2}$ (equation (18)), while a contact crack model would imply a scaling of the same quantity with $G_{IC}^{3/2}$ (equation (22)). These dependencies can inspire further connections between macroscopic processes involving particle breakage and the micro-scale multi-physics of grain fracture. Much research has indeed been devoted to study the fracture of geomaterials under environmental perturbations such as changes in relative humidity and temperature (Atkinson, 1982; Nara et al., 2012). The energy-based scaling law proposed in this study can therefore bridge well characterized fracture properties of soil-forming minerals with macroscopic observations of environmentally assisted crushing in granular soils (Oldecop and Alonso, 2007; Zhang and Buscarnera, 2015). Therefore, the proposed approach sets a new vision to tackle the challenges posed by numerous modern underground technologies, which often imply the exposure of geomaterials to extreme

Accepted Manuscript

environments (e.g., high pressures, temperatures, and chemically active pore fluids; (Buscarnera and Einav, 2012; Buscarnera, 2012)).

CONCLUSIONS

We have proposed an upscaling law to bridge the micromechanics of grain fracture with the macroscopic yielding of granular soils subjected to large compressive stresses. The theory relies on a simple linear scaling between the energy input required to fracture individual grains and the energy associated with the collective crushing of an assembly composed of particles with the same characteristics. Several grain-scale models of contact deformation (e.g., linear, Hertzian, and conical contacts) and grain fracture (e.g., failure at centred cracks, at contact cracks, and Weibull-type failure) have been used to validate such hypotheses. The proposed strategy has been validated against data for various sands that displayed significant grainsize effects in terms of both particle-scale and continuum-scale properties (e.g., forces at grain failure, as well as macroscopic yield pressure). The performance of both deterministic and statistical models has been discussed. It has been shown that the combination of the Weibull's statistics for particle strength with the Hertzian contact theory provides the best performance in predicting the effect of the grainsize on various indicators of particle failure, spanning from the tensile strength of the grains to the critical energy thresholds at the onset of fracture. In addition, it has been shown that such combination of particle scale models is able to predict accurately the effect of the grainsize in terms of yield pressure, which for the case of quartz sands was captured satisfactorily only by using data about the size dependence of the particle strength. It has also been found that the grainsize effect predicted through deterministic fracture models can explain the large

Accepted Manuscript

data scatter emerging from experiments. In particular, it has been found that the broad range of values measured for particle strength and yielding stresses is well captured by the predictions of the two grain fracture models considered in this study (i.e., failure by propagation of centred cracks and contact cracks, respectively). Furthermore, a comparison of the predictions from deterministic and statistical models has indicated that the data scatter can be explained in statistical terms, with the range of variation of the two deterministic theories being covered by values of Weibull moduli spanning between $w = 2$ and $w = 6$ (a range that is typical of granular materials and that here has been shown to provide the same power-law dependencies retrieved from the contact crack and the centred crack models, respectively).

The integration of breakage and fracture mechanics discussed in this paper opens new avenues to extrapolate measurements obtained from small-scale laboratory models of granular systems to realistic field conditions. In addition, the theory is susceptible to future generalizations incorporating the multi-physics of grain fracture and can therefore provide new theoretical bases to estimate the effect of widely variable particle sizes in large-scale applications where the direct testing of realistic geometric and environmental conditions is not feasible, such as rockfill engineering and mining technologies.

ACKNOWLEGMENTS

G.B. wishes to thank the support of the U. S. National Science Foundation (project CMMI-1351534) and of the American Chemical Society (project PRF-55647-ND8). I.E. wishes to thank the Australian Research Council for support through project DP130101291.

REFERENCES

Accepted Manuscript

Alonso, E., Olivella, S. & Pinyol, N. (2005) A review of Beliche dam. *Geotechnique* **55(4)**:267-285.

Alonso, E., Tapias, M. & Gili, J. (2012) Scale effects in rockfill behaviour. *Géotechnique Letters* **2(July-September)**:155-160.

Atkinson, B. K. (1982) Subcritical crack propagation in rocks: theory, experimental results and applications. *Journal of Structural Geology* **4(1)**:41-56.

Brzesowsky, R., Spiers, C., Peach, C. & Hangx, S. (2011) Failure behavior of single sand grains: Theory versus experiment. *Journal of Geophysical Research: Solid Earth (1978–2012)* **116(B6)**.

Brzesowsky, R., Spiers, C., Peach, C. & Hangx, S. (2014) Time‐independent compaction behavior of quartz sands. *Journal of Geophysical Research: Solid Earth* **119(2)**:936-956.

Buscarnera, G. (2012). A conceptual model for the chemo-mechanical degradation of granular geomaterials. *Géotechnique Letters*, 2, 149-154.

Buscarnera, G., & Einav, I. (2012). The yielding of brittle unsaturated granular soils. *Géotechnique*, 62(2), 147-160.

Coop, M., Sorensen, K., Freitas, T. B. & Georgoutsos, G. (2004) Particle breakage during shearing of a carbonate sand. *Geotechnique* **54(3)**:157-163.

Einav, I. (2007a) Breakage mechanics—part I: theory. *Journal of the Mechanics and Physics of Solids* **55(6)**:1274-1297.

Einav, I. (2007b) Breakage mechanics—Part II: Modelling granular materials. *Journal of the Mechanics and Physics of Solids* **55(6)**:1298-1320.

Einav, I. (2007c) Fracture propagation in brittle granular matter. *Proceedings of the Royal Society A: Mathematical, Physical and Engineering Science* **463(2087)**:3021-3035.

Frank, F. & Lawn, B. (1967) On the theory of Hertzian fracture. *Proceedings of the Royal Society of London. Series A. Mathematical and Physical Sciences* **299(1458)**:291-306.

Frossard, E., Hu, W., Dano, C. & Hicher, P.-Y. (2012) Rockfill shear strength evaluation: a rational method based on size effects. *Geotechnique* **62(5)**:415-427.

Goddard, J. (1990) Nonlinear elasticity and pressure-dependent wave speeds in granular media. *Proceedings of the Royal Society of London. Series A: Mathematical and Physical Sciences* **430(1878)**:105-131.

Griffith, A. A. (1921) The phenomena of rupture and flow in solids. *Philosophical transactions of the royal society of london. Series A, containing papers of a mathematical or physical character*:163-198.

Guimaraes, M., Valdes, J., Palomino, A. & Santamarina, J. (2007) Aggregate production: fines generation during rock crushing. *International journal of mineral processing* **81(4)**:237-247.

Hiramatsu, Y. & Oka, Y. (1966) Determination of the tensile strength of rock by a compression test of an irregular test piece. In *International Journal of Rock Mechanics and Mining Sciences & Geomechanics Abstracts*.) Elsevier, vol. 3, pp. 89-90.

Jaeger, J. (1967) Failure of rocks under tensile conditions. In *International Journal of Rock Mechanics and Mining Sciences & Geomechanics Abstracts*.) Elsevier, vol. 4, pp. 219-227.

Jäger, J. (1999) Uniaxial deformation of a random packing of particles. *Archive of Applied Mechanics* **69(3)**:181-203.

Kassir, M. & Sih, G. C. (1966) Three-dimensional stress distribution around an elliptical crack under arbitrary loadings. *Journal of Applied Mechanics* **33(3)**:601-611.

Lade, P. V., Yamamuro, J. A. & Bopp, P. A. (1996) Significance of particle crushing in granular materials. *Journal of Geotechnical Engineering* **122(4)**:309-316.

Lee, D.-M. (1992) The angles of friction of granular fills.) University of Cambridge.

Lim, W. L., Mcdowell, G. R. & Collop, A. C. (2004) The application of Weibull statistics to the strength of railway ballast. *Granular Matter* **6(4)**:229-237.

Accepted Manuscript

Mcdowell, G. & Amon, A. (2000) The application of weibull statistics to the fracture of soil particles. *Soils and foundations* **40(5)**:133-141.

Mcdowell, G. & Bolton, M. (1998) On the micromechanics of crushable aggregates. *Geotechnique* **48(5)**:667-679.

Mcdowell, G. (2002) On the yielding and plastic compression of sand. *Soils and foundations* **42(1)**:139-145.

Mcdowell, G. R. & De Bono, J. P. (2013) On the micro mechanics of one-dimensional normal compression. *Geotechnique* **63**.

Mcdowell, G., Bolton, M. & Robertson, D. (1996) The fractal crushing of granular materials. *Journal of the Mechanics and Physics of Solids* **44(12)**:2079-2101.

Mogi, K. (1962) The influence of the dimensions of specimens on the fracture strength of rocks. *Bulletin of the Earthquake Research Institute* **40**, 175-185.

Montgomery, C. & Steanson, R. (1985) Proppant selection: the key to successful fracture stimulation. *Journal of petroleum technology* **37(12)**:2,163-2,172.

Nakata, A., Hyde, M. & Hyodo, H. (1999) A probabilistic approach to sand particle crushing in the triaxial test. *Geotechnique* **49(5)**:567-583.

Nakata, Y., Kato, Y., Hyodo, M., Hyde, A. F. L. & Murata, H. (2001) One-dimensional compression behaviour of uniformly graded sand related to single particle crushing strength. *Soils and foundations* **41(2)**:39-51.

Nara, Y., Morimoto, K., Hiroyoshi, N., Yoneda, T., Kaneko, K. & Benson, P. M. (2012) Influence of relative humidity on fracture toughness of rock: implications for subcritical crack growth. *International Journal of Solids and Structures* **49(18)**:2471-2481.

Nguyen, G. D. & Einav, I. (2009) The energetics of cataclasis based on breakage mechanics. *Pure and Applied Geophysics* **166(10)**: 1693–1724.

Oldecop, L. A. & Alonso, E. (2007) Theoretical investigation of the time-dependent behaviour of rockfill. *Geotechnique* **57(3)**:289-301.

Ovalle, C., Frossard, E., Dano, C., Hu, W., Maiolino, S. & Hicher, P.-Y. (2014) The effect of size on the strength of coarse rock aggregates and large rockfill samples through experimental data. *Acta Mechanica* **225(8)**:2199-2216.

Rothenburg, L. & Bathurst, R. (1989) Analytical study of induced anisotropy in idealized granular materials. *Geotechnique* **39(4)**:601-614.

Russell, A. R. & Einav, I. (2013) Energy dissipation from particulate systems undergoing a single particle crushing event. *Granular Matter* **15(3)**:299-314.

Ryu, H. J. & Saito, F. (1991) Single particle crushing of nonmetallic inorganic brittle materials. *Solid state ionics* **47(1)**:35-50.

Salman, A. & Gorham, D. (2000) The fracture of glass spheres. *Powder technology* **107(1)**:179-185.

Shipway, P. & Hutchings, I. (1993) Fracture of brittle spheres under compression and impact loading. I. Elastic stress distributions. *Philosophical Magazine A* **67(6)**:1389-1404.

Tavares, L. & King, R. (1998) Single-particle fracture under impact loading. *International journal of mineral processing* **54(1)**:1-28.

Timoshenko, S. & Goodier, J. (1951) Theory of elasticity. *New York*:412.

Weibull, W. (1951). A Statistical Distribution Function of Wide Applicability. *Journal of Applied Mechanics*, **13**, 293-297.

Yang, Z., Jardine, R., Zhu, B., Foray, P. & Tsuha, C. (2010) Sand grain crushing and interface shearing during displacement pile installation in sand. *Geotechnique* **60(6)**:469-482.

Yashima, S., Kanda, Y. & Sano, S. (1987) Relationships between particle size and fracture energy or impact velocity required to fracture as estimated from single particle crushing. *Powder technology* **51(3)**:277-282.

Accepted Manuscript

Zhang, C., Nguyen, G. & Einav, I. (2012) The end-bearing capacity of piles penetrating into crushable soils. *Geotechnique* **63(5)**:341-354.

Zhang, J., Wong, T. F. & Davis, D. M. (1990) Micromechanics of pressure‐induced grain crushing in porous rocks. *Journal of Geophysical Research: Solid Earth (1978–2012)* **95(B1)**:341-352.

Zhang, Y. & Buscarnera, G. (2014) Grainsize dependence of clastic yielding in unsaturated granular soils. *Granular Matter* **16(4)**:469-483.

Zhang, Y. D., & Buscarnera, G. (2015). Prediction of breakage-induced couplings in unsaturated granular soils. *Geotechnique* **65(2)**, 135 –140.

Accepted Manuscript